

Epigenome editing by a CRISPR-Cas9-based acetyltransferase activates genes from promoters and enhancers

Isaac B Hilton^{1,2}, Anthony M D'Ippolito^{2,3}, Christopher M Vockley^{2,4}, Pratiksha I Thakore^{1,2}, Gregory E Crawford^{2,5}, Timothy E Reddy^{2,6} & Charles A Gersbach^{1,2,7}

Technologies that enable targeted manipulation of epigenetic marks could be used to precisely control cell phenotype or interrogate the relationship between the epigenome and transcriptional control. Here we describe a programmable, CRISPR-Cas9-based acetyltransferase consisting of the nuclease-null dCas9 protein fused to the catalytic core of the human acetyltransferase p300. The fusion protein catalyzes acetylation of histone H3 lysine 27 at its target sites, leading to robust transcriptional activation of target genes from promoters and both proximal and distal enhancers. Gene activation by the targeted acetyltransferase was highly specific across the genome. In contrast to previous dCas9-based activators, the acetyltransferase activates genes from enhancer regions and with an individual guide RNA. We also show that the core p300 domain can be fused to other programmable DNA-binding proteins. These results support targeted acetylation as a causal mechanism of transactivation and provide a robust tool for manipulating gene regulation.

A central challenge in functional genomics is to develop technologies for precise manipulation of individual loci. Projects such as ENCODE¹ and the Roadmap Epigenomics Project² have identified millions of epigenetic marks across the human genome for many human cell types and tissues. Studying the function of those marks, however, has been largely limited to determining statistical associations with gene expression. Technologies for targeted direct manipulation of epigenetic marks are needed to transform association-based findings into mechanistic principles of gene regulation. Such advances have the potential to benefit human health by enabling new platforms for disease modeling, drug screening, gene therapy and cell lineage specification. Small-molecule drugs, such as inhibitors of histone deacetylases or DNA methyltransferases, alter the epigenome and transcriptome globally and cannot target individual loci. Fusions of epigenome-modifying enzymes to programmable DNA-binding proteins, such as zinc finger proteins and transcription activator-like effectors (TALEs), are effective at achieving targeted DNA methylation and hydroxymethylation, and histone demethylation, methylation and deacetylation^{3–8}. However, a method for targeted histone acetylation, which is strongly associated with active gene regulatory elements and enhancers, has not been described. In addition, the CRISPR-Cas9 (clustered, regularly interspaced, short palindromic repeat–CRISPR-associated protein) genome engineering tool^{9,10}, which can be readily targeted to loci of interest, has not yet been extensively applied to epigenome editing.

The Cas9 nuclease can be directed to specific genomic loci using complementarity between an engineered guide RNA (gRNA) and the target site^{11–13}. The enzymatic activity of the Cas9 nuclease can be abolished by mutation of the RuvC and HNH domains, generating the nuclease-null deactivated Cas9 (dCas9)¹². Fused to repression domains, such as the KRAB domain, or to activation domains, such as oligomers of the herpes simplex viral protein 16 (VP16), dCas9 can function as a synthetic transcriptional regulator^{14–21}. However, dCas9 activators have limitations, including the need for multiple activation domains^{14,20,22,23} or combinations of gRNAs^{16,17} to achieve high levels of gene induction by synergistic effects between activation domains^{24,25}. Moreover, the activator domains used in these engineered transcriptional factors, such as the VP16 tetramer VP64 (ref. 26), act as scaffolds for recruiting multiple components of the preinitiation complex^{27,28} and do not enzymatically modulate the chromatin state directly. This indirect method of epigenetic remodeling does not allow testing of the role of specific epigenetic marks and may not be as potent as direct alteration of epigenetic states. We hypothesized that recruitment of an acetyltransferase by dCas9 to a genomic target site would directly modulate the epigenome and activate nearby gene expression. To this end, we designed a fusion protein of dCas9 with the catalytic histone acetyltransferase (HAT) core domain of the human E1A-associated protein p300 (ref. 29), a highly conserved acetyltransferase involved in a wide range of cellular processes^{30,31}.

¹Department of Biomedical Engineering, Duke University, Durham, North Carolina, USA. ²Center for Genomic & Computational Biology, Duke University, Durham, North Carolina, USA. ³University Program in Genetics and Genomics, Duke University Medical Center, Durham, North Carolina, USA. ⁴Department of Cell Biology, Duke University Medical Center, Durham, North Carolina, USA. ⁵Department of Pediatrics, Division of Medical Genetics, Duke University Medical Center, Durham, North Carolina, USA. ⁶Department of Biostatistics & Bioinformatics, Duke University Medical Center, Durham, North Carolina, USA. ⁷Department of Orthopaedic Surgery, Duke University Medical Center, Durham, North Carolina, USA. Correspondence should be addressed to T.E.R. (tim.reddy@duke.edu) or C.A.G. (charles.gersbach@duke.edu).

Received 23 December 2014; accepted 16 March 2015; published online 6 April 2015; doi:10.1038/nbt.3199

We demonstrate that this easily programmable approach facilitates robust control of the epigenome and downstream gene expression.

RESULTS

A dCas9 fusion to the p300 HAT domain activates target genes

We fused the full-length human p300 protein to dCas9 (dCas9^{FLp300}; **Fig. 1a,b**) and assayed its capacity for transactivation by transient co-transfection of human HEK293T cells with four gRNAs targeting the endogenous promoters of *IL1RN*, *MYOD* (also known as *MYOD1*) and *OCT4* (also known as *POU5F1*; **Fig. 1c**). We used a combination of four gRNAs targeting each promoter based on our and others' previous observations that multiple gRNAs at a single promoter are necessary for robust gene activation^{14–22}. dCas9^{FLp300} was well-expressed and induced modest activation above background compared to the canonical dCas9 activator fused to the VP64 acidic activation domain (dCas9^{VP64}; **Fig. 1a–c**). The full-length p300 protein is a promiscuous acetyltransferase, which interacts with a multitude of endogenous proteins, largely through its terminus^{29,31}. To mitigate these interactions we isolated the contiguous region of full-length p300 (2,414 amino acids) solely required for inherent HAT activity (amino acids 1,048–1,664), known as the p300 HAT core domain (p300 Core)²⁹. When fused to the C terminus of dCas9 (dCas9^{p300 Core}; **Fig. 1a,b**) the p300 Core domain induced high levels of transcription from endogenous gRNA-targeted promoters (**Fig. 1c**). When targeted to the *IL1RN* and *MYOD* promoters, the dCas9^{p300 Core} fusion displayed significantly higher levels of transactivation than dCas9^{VP64} ($P = 0.0124$ and 0.0394 , respectively; **Fig. 1c**). These dCas9-effector fusion proteins were expressed at similar levels (**Fig. 1b** and **Supplementary Fig. 1**) indicating that the observed differences reflect the distinct transactivation capacity of each construct. In addition, no changes to target gene expression were observed when the effector fusions were transfected without gRNAs (**Supplementary Fig. 2**). To confirm that the p300 Core acetyltransferase activity was responsible for gene transactivation using the dCas9^{p300 Core} fusion, we screened a panel of dCas9^{p300 Core} HAT-domain mutant fusion proteins (**Supplementary Fig. 1**)²⁹. A single inactivating amino acid substitution within the HAT core domain (WT residue D1399 of

full-length p300) of dCas9^{p300 Core} (dCas9^{p300 Core} (D1399Y); **Fig. 1a**) abolished the transactivation capacity of the fusion protein (**Fig. 1c**), demonstrating that intact p300 Core acetyltransferase activity was required for dCas9^{p300 Core}-mediated transactivation.

dCas9^{p300 Core} activates genes from proximal and distal enhancers

Although there are many published examples of genes being activated with engineered transcription factors targeted to promoters, inducing gene expression from other distal regulatory elements has been limited, particularly for dCas9-based activators^{32–35}. Given the role and localization of p300 at endogenous enhancers^{36,37}, we hypothesized that the dCas9^{p300 Core} would effectively induce transcription from distal regulatory regions with appropriately targeted gRNAs. We targeted the distal regulatory region (DRR) and core enhancer (CE) of the human *MYOD* locus³⁸ through co-transfection of four gRNAs targeted to each region and either dCas9^{VP64} or dCas9^{p300 Core} (**Fig. 2a**). Compared to a mock-transfected control, dCas9^{VP64} did not lead to any induction when targeted to the *MYOD* DRR or CE region. In contrast, dCas9^{p300 Core} induced significant transcription when targeted to either *MYOD* regulatory element with corresponding gRNAs ($P = 0.0115$ and 0.0009 for the CE and DRR regions, respectively). We also targeted the upstream proximal (PE) and distal enhancer (DE) regions of human *OCT4* (ref. 39) by co-transfection of six gRNAs and either dCas9^{VP64} or dCas9^{p300 Core} (**Fig. 2b**). dCas9^{p300 Core} induced significant transcription from these regions ($P \leq 0.0001$ and $P = 0.003$ for the DE and PE, respectively), whereas dCas9^{VP64} was unable to activate *OCT4* above background levels when targeted to either the PE or DE regions.

The well-characterized mammalian β -globin locus control region (LCR) orchestrates transcription of the downstream hemoglobin genes; hemoglobin epsilon 1 (*HBE*, also known as *HBE1*, from ~11 kb), hemoglobin gamma 1 and 2 (*HBG*, also known as *HBG1*, from ~30 kb), hemoglobin delta (*HBD*, from ~46 kb) and hemoglobin beta (*HBB*, from ~54 kb) (**Fig. 2c**)^{35,40}. DNase hypersensitive sites within the β -globin LCR serve as docking sites for transcriptional and chromatin modifiers, including p300 (ref. 41), which coordinate distal target gene expression. We designed four gRNAs targeting the

DNase hypersensitive site 2 within the LCR enhancer region (HS2 enhancer). These four HS2-targeted gRNAs were co-transfected with dCas9, dCas9^{VP64}, dCas9^{p300 Core} or

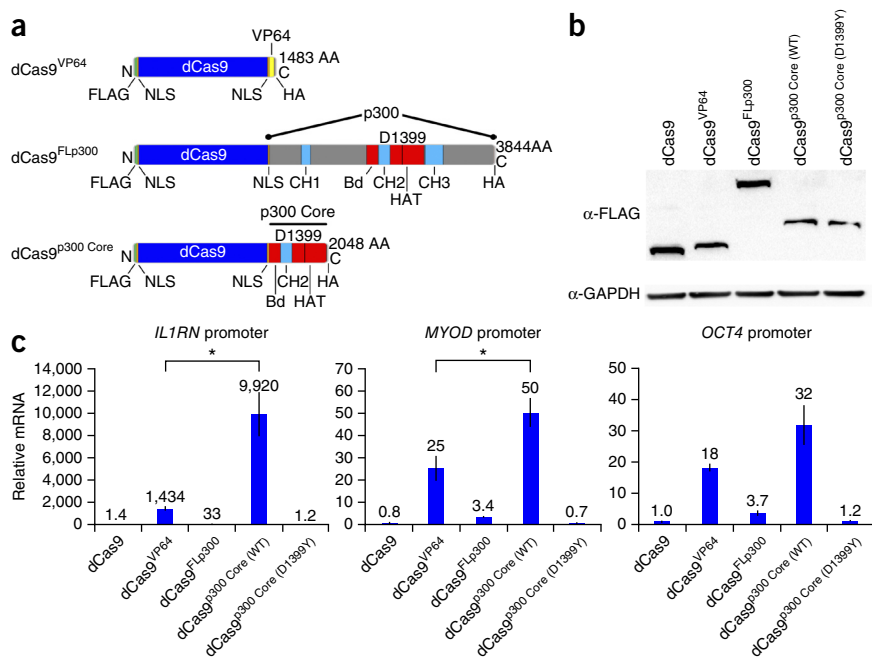
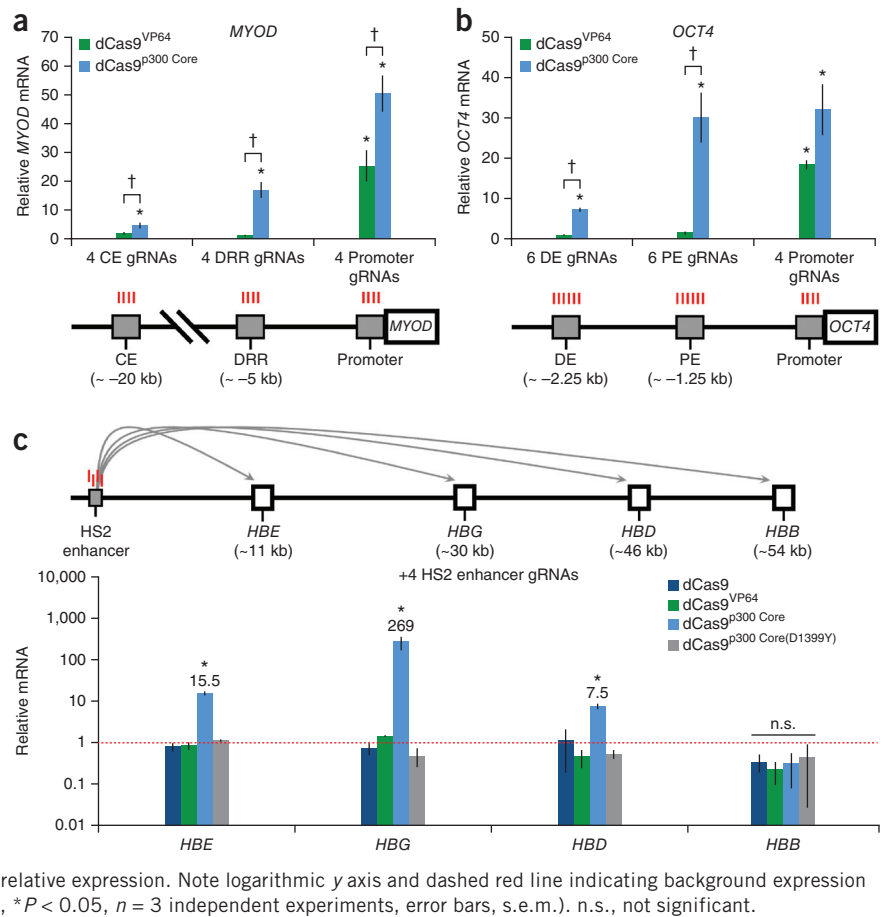


Figure 1 The dCas9^{p300 Core} fusion protein activates transcription of endogenous genes from proximal promoter regions. **(a)** Schematic of dCas9 fusion proteins dCas9^{VP64}, dCas9^{FLp300} and dCas9^{p300 Core}. *S. pyogenes* dCas9 contains nuclease-inactivating mutations D10A and H840A. The D1399 catalytic residue in the p300 HAT domain is indicated. **(b)** Western blot showing expression of dCas9 fusion proteins and GAPDH in co-transfected cells (full blot shown in **Supplementary Fig. 1c**). **(c)** Relative mRNA expression of *IL1RN*, *MYOD* and *OCT4*, determined by qRT-PCR, by the indicated dCas9 fusion protein co-transfected with four gRNAs targeted to each promoter region (Tukey-test, $*P < 0.05$, $n = 3$ independent experiments each; error bars, s.e.m.). Numbers above bars indicate mean relative expression. FLAG, epitope tag; NLS, nuclear localization signal; HA, hemagglutinin epitope tag; CH, cysteine-histidine-rich region; Bd, bromodomain; HAT, histone acetyltransferase domain.

Figure 2 The dCas9^{p300} Core fusion protein activates transcription of endogenous genes from distal enhancer regions. **(a)** Relative *MYOD* mRNA production in cells co-transfected with a pool of gRNAs targeted to either the proximal or distal regulatory regions and dCas9^{VP64} or dCas9^{p300} Core, promoter data from **Figure 1c** (Tukey-test, $*P < 0.05$ compared to mock-transfected cells; Tukey test $\dagger P < 0.05$ between dCas9^{p300} Core and dCas9^{VP64}, $n = 3$ independent experiments; error bars, s.e.m.). The human *MYOD* locus is schematically depicted with corresponding gRNA locations in red. CE, MyoD core enhancer; DRR, MyoD distal regulatory region. **(b)** Relative *OCT4* mRNA production in cells co-transfected with a pool of gRNAs targeted to the proximal and distal regulatory regions and dCas9^{VP64} or dCas9^{p300} Core, promoter data from **Figure 1c** (Tukey-test, $*P < 0.05$ compared to mock-transfected cells, Tukey test $\dagger P < 0.05$ between dCas9^{p300} Core and dCas9^{VP64}, $n = 3$ independent experiments; error bars, s.e.m.). The human *OCT4* locus is schematically depicted with corresponding gRNA locations in red. DE, Oct4 distal enhancer; PE, Oct4 proximal enhancer. **(c)** The human β -globin locus is schematically depicted with approximate locations of the hypersensitive site 2 (HS2) enhancer region and downstream genes (*HBE*, *HBG*, *HBD* and *HBB*). Corresponding HS2 gRNA locations are shown in red. Relative mRNA production from distal genes in cells co-transfected with four gRNAs targeted to the HS2 enhancer and the indicated dCas9 proteins. Numbers above bars indicate mean relative expression. Note logarithmic y axis and dashed red line indicating background expression (Tukey test among conditions for each β -globin gene, $*P < 0.05$, $n = 3$ independent experiments, error bars, s.e.m.). n.s., not significant.



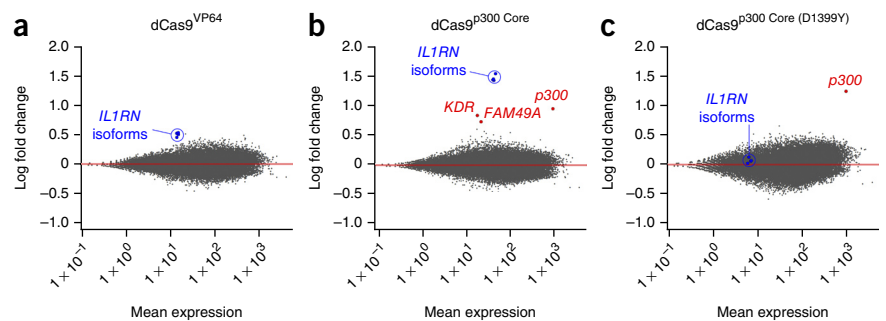
dCas9^{p300} Core (D1399Y), and the resulting mRNA production from *HBE*, *HBG*, *HBD* and *HBB* was assayed (**Fig. 2c**). dCas9, dCas9^{VP64} and dCas9^{p300} Core (D1399Y) did not transactivate any downstream genes when targeted to the HS2 enhancer. In contrast, targeting of dCas9^{p300} Core to the HS2 enhancer led to significant expression of the downstream *HBE*, *HBG* and *HBD* genes ($P \leq 0.0001$, 0.0056 , and 0.0003 between dCas9^{p300} Core and mock-transfected cells for *HBE*, *HBG* and *HBD*, respectively). Overall, *HBD* and *HBE* appeared relatively less responsive to synthetic p300 Core-mediated activation from the HS2 enhancer; a finding consistent with lower rates of general transcription from these two genes across several cell lines (**Supplementary Fig. 3**). Nevertheless, with the exception of the most distal *HBB* gene, dCas9^{p300} Core activated transcription from downstream genes when targeted to all characterized enhancer regions assayed, a capability

not observed for dCas9^{VP64}. Together, these results demonstrate that dCas9^{p300} Core is a potent programmable transcription factor that can be used to regulate gene expression from a variety of promoter-proximal and promoter-distal locations.

Gene activation by dCas9^{p300} Core is highly specific

Recent reports indicate that dCas9 may have widespread off-target binding events in mammalian cells in combination with some gRNAs^{42,43}, which could potentially lead to off-target changes in gene expression. To assess the transcriptional specificity of the dCas9^{p300} Core fusion protein we performed transcriptome profiling by RNA-seq in cells co-transfected with four *IL1RN*-targeted gRNAs and either dCas9, dCas9^{VP64}, dCas9^{p300} Core or dCas9^{p300} Core (D1399Y). Genome-wide transcriptional changes were compared between

Figure 3 dCas9^{p300} Core-targeted transcriptional activation is specific and robust. **(a–c)** MA plots generated from DESeq2 analysis of genome-wide RNA-seq data from HEK293T cells transiently co-transfected with dCas9^{VP64} **(a)** dCas9^{p300} Core **(b)** or dCas9^{p300} Core (D1399Y) **(c)** and four *IL1RN* promoter-targeting gRNAs compared to HEK293T cells transiently co-transfected with dCas9 and four *IL1RN* promoter-targeting gRNAs. mRNAs corresponding to *IL1RN* isoforms are shown in blue and circled in each panel. Red-labeled points in **b** and **c** correspond to off-target transcripts significantly enriched after multiple hypothesis testing (*KDR* (FDR = 1.4×10^{-3}); *FAM49A* (FDR = 0.04); *p300* (FDR = 1.7×10^{-4}) in **b**; and *p300* (FDR = 1.5×10^{-5}) in **c**).



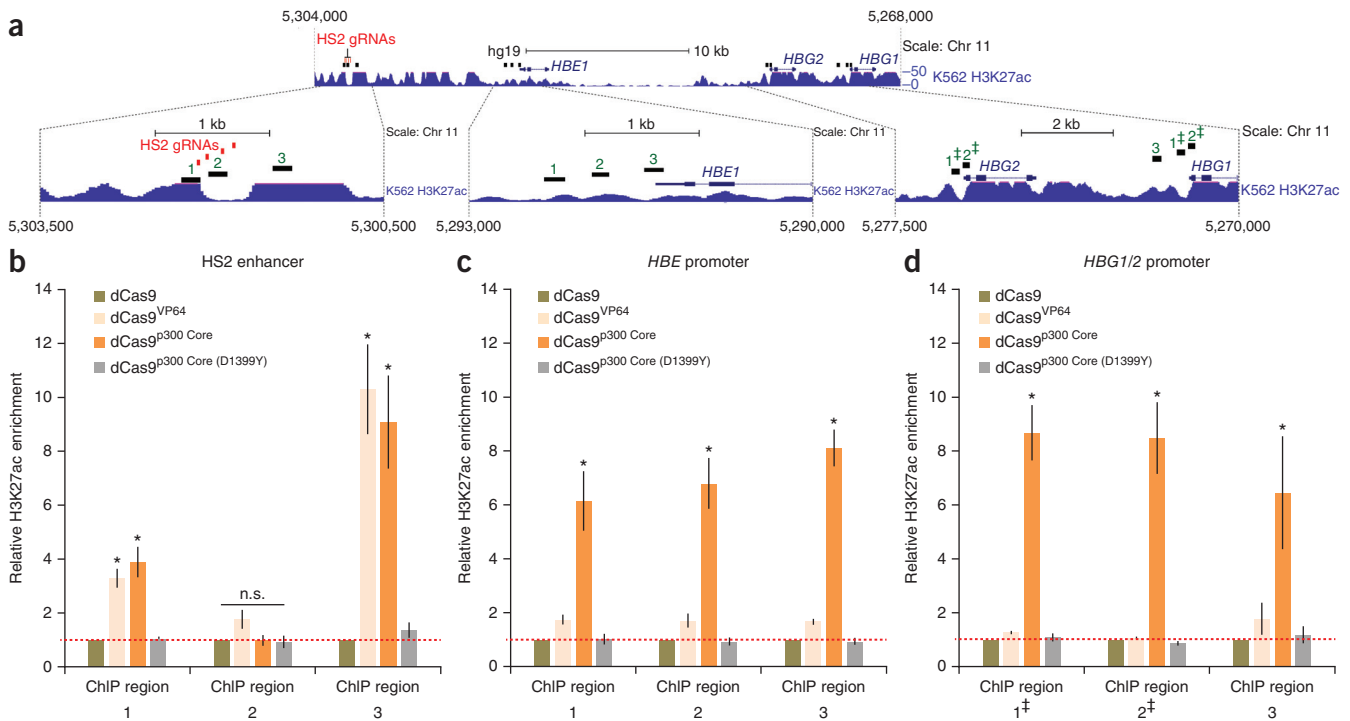


Figure 4 The dCas9^{p300 Core} fusion protein acetylates chromatin at a targeted enhancer and corresponding downstream genes. (a) The region encompassing the human β -globin locus on chromosome 11 (5,304,000–5,268,000; GRCh37/hg19 assembly) is shown. HS2 gRNA target locations are indicated in red and ChIP-qPCR amplicon regions are depicted in black with corresponding green numbers. ENCODE/Broad Institute H3K27ac enrichment signal in K562 cells is shown for comparison. Magnified insets for the HS2 enhancer, *HBE* promoter and *HBG1/2* promoter regions are displayed below. (b–d) H3K27ac ChIP-qPCR enrichment (relative to dCas9; red dashed line) at the HS2 enhancer (b), *HBE* promoter (c) and *HBG1/2* promoters (d) in cells co-transfected with four gRNAs targeted to the HS2 enhancer and the indicated dCas9 fusion protein. *HBG* ChIP amplicons 1 and 2 amplify redundant sequences at the *HBG1* and *HBG2* promoters (denoted by ‡). Tukey test among conditions for each ChIP-qPCR region, * $P < 0.05$ ($n = 3$ independent experiments; error bars, s.e.m.).

dCas9 with no fused effector domain and either dCas9^{VP64}, dCas9^{p300 Core} or dCas9^{p300 Core (D1399Y)} (Fig. 3). Whereas both dCas9^{VP64} and dCas9^{p300 Core} upregulated all four *IL1RN* isoforms, only the effects of dCas9^{p300 Core} reached genome-wide significance (Fig. 3a,b and Supplementary Table 1; $P = 4.9 \times 10^{-4}$ to 2.7×10^{-3} for dCas9^{VP64}; $P = 1.5 \times 10^{-19}$ to 4.9×10^{-17} for dCas9^{p300 Core}). In contrast, dCas9^{p300 Core (D1399Y)} did not significantly induce any *IL1RN* expression (Fig. 3c; $P > 0.5$ for all four *IL1RN* isoforms). Comparative analysis to dCas9 revealed limited dCas9^{p300 Core} off-target gene induction, with only two transcripts induced significantly above background at a false discovery rate (FDR) $< 5\%$: *KDR* (FDR = 1.4×10^{-3}) and *FAM49A* (FDR = 0.04) (Fig. 3b and Supplementary Table 1). We also found increased expression of *p300* mRNA in cells transfected with dCas9^{p300 Core} and dCas9^{p300 Core (D1399Y)}. This finding is most likely explained by RNA-seq reads mapping to mRNA from the transiently transfected p300 core fusion domains. Thus the dCas9^{p300 Core} fusion displayed high genome-wide targeted transcriptional specificity and robust gene induction of all four targeted *IL1RN* isoforms.

dCas9^{p300 Core} acetylates H3K27 at enhancers and promoters

Activity of regulatory elements correlates with covalent histone modifications, such as acetylation and methylation^{1,2}. Of those histone modifications, acetylation of lysine 27 on histone H3 (H3K27ac) is one of the most widely documented indicators of enhancer activity^{29–31,36,37}. Acetylation of H3K27 is catalyzed by p300 and is also correlated with endogenous p300 binding profiles^{36,37}. Therefore, we used H3K27ac enrichment as a measurement of

relative dCas9^{p300 Core}-mediated acetylation at the genomic target site. To quantify targeted H3K27 acetylation by dCas9^{p300 Core}, we performed chromatin immunoprecipitation with an anti-H3K27ac antibody followed by quantitative PCR (ChIP-qPCR) in HEK293T cells co-transfected with four HS2 enhancer-targeted gRNAs and either dCas9, dCas9^{VP64}, dCas9^{p300 Core} or dCas9^{p300 Core (D1399Y)} (Fig. 4). We analyzed three amplicons at or around the target site in the HS2 enhancer or within the promoter regions of the *HBE* and *HBG* genes (Fig. 4a). Notably, H3K27ac is enriched in each of these regions in the human K562 erythroid cell line, which has a high level of globin gene expression (Fig. 4a). We observed significant H3K27ac enrichment at the HS2 enhancer target locus compared to treatment with dCas9 in both the dCas9^{VP64} ($P = 0.0056$ for ChIP Region 1 and $P = 0.0029$ for ChIP Region 3) and dCas9^{p300 Core} ($P = 0.0013$ for ChIP Region 1 and $P = 0.0069$ for ChIP Region 3) co-transfected samples (Fig. 4b). A similar trend of H3K27ac enrichment was also observed when targeting the *IL1RN* promoter with dCas9^{VP64} or dCas9^{p300 Core} (Supplementary Fig. 4). In contrast to these increases in H3K27ac at the target sites by both dCas9^{VP64} and dCas9^{p300 Core}, robust enrichment in H3K27ac at the HS2-regulated *HBE* and *HBG* promoters was observed only with dCas9^{p300 Core} treatment (Fig. 4c,d). Together these results demonstrate that dCas9^{p300 Core} uniquely catalyzes H3K27ac enrichment at gRNA-targeted loci and at enhancer-targeted distal promoters. Therefore, the acetylation established by dCas9^{p300 Core} at HS2 may catalyze enhancer activity in a manner distinct from direct recruitment of preinitiation complex components by dCas9^{VP64} (refs. 27,28), as indicated by the distal activation of the *HBE*, *HBG*

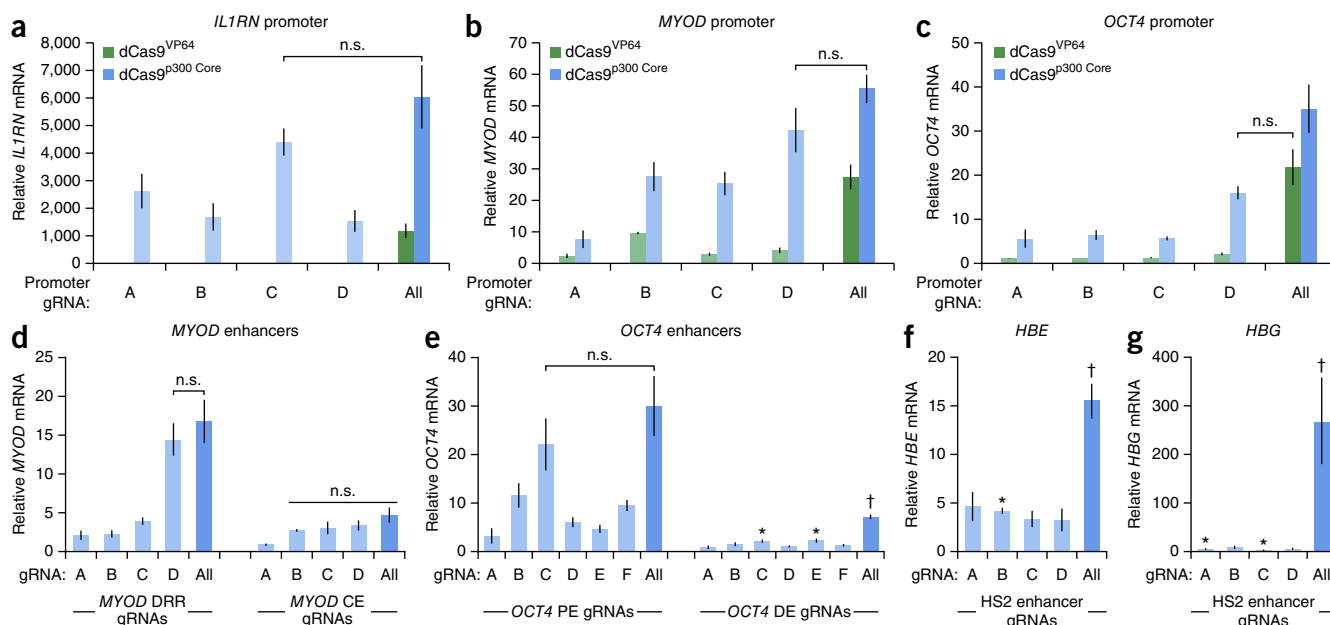


Figure 5 The dCas9^{p300Core} fusion protein activates transcription of endogenous genes from regulatory regions with a single gRNA. (**a–c**) Relative *IL1RN* (**a**), *MYOD* (**b**) or *OCT4* (**c**) mRNA produced from cells co-transfected with dCas9^{p300Core} or dCas9^{VP64} and gRNAs targeting respective promoters ($n = 3$ independent experiments, error bars, s.e.m.). (**d,e**) Relative *MYOD* (**d**) or *OCT4* (**e**) mRNA produced from cells co-transfected with dCas9^{p300Core} and indicated gRNAs targeting the indicated *MYOD* or *OCT4* enhancers ($n = 3$ independent experiments; error bars, s.e.m.). DRR, *MYOD* distal regulatory region; CE, *MYOD* core enhancer; PE, *OCT4* proximal enhancer; DE, *OCT4* distal enhancer. (Tukey test between dCas9^{p300Core} and single *OCT4* DE gRNAs compared to mock-transfected cells, * $P < 0.05$; Tukey test among dCas9^{p300Core} and *OCT4* DE gRNAs compared to All, † $P < 0.05$.) (**f,g**) Relative *HBE* (**f**) or *HBG* (**g**) mRNA production in cells co-transfected with dCas9^{p300Core} and the indicated gRNAs targeted to the HS2 enhancer (Tukey test between dCas9^{p300Core} and single HS2 gRNAs compared to mock-transfected cells, * $P < 0.05$; Tukey test among dCas9^{p300Core} and HS2 single gRNAs compared to All, † $P < 0.05$, $n = 3$ independent experiments; error bars, s.e.m.). HS2, β -globin locus control region hypersensitive site 2; n.s., not significant using Tukey test.

and *HBD* genes from the HS2 enhancer by dCas9^{p300Core} but not by dCas9^{VP64} (Fig. 2c and Supplementary Fig. 3).

dCas9^{p300Core} activates genes with a single gRNA

Robust transactivation using dCas9-effector fusion proteins currently relies upon the application of multiple gRNAs, multiple effector domains or both^{14–22,24,25}. Transcriptional activation could be simplified with the use of single gRNAs in tandem with a single dCas9-effector fusion. This would also facilitate multiplexing distinct target genes and the incorporation of additional functionalities into the system. We compared the transactivation potential of dCas9^{p300Core} with single gRNAs and four pooled gRNAs targeting the *IL1RN*, *MYOD* and *OCT4* promoters (Fig. 5a–c). Substantial activation was observed upon co-transfection of the dCas9^{p300Core} and a single gRNA for each promoter tested. For the *IL1RN* and *MYOD* promoters, there was no significant difference between the pooled gRNAs and the best individual gRNA (Fig. 5a–b; *IL1RN* gRNA “C”, $P = 0.78$; *MYOD* gRNA “D”, $P = 0.26$). Although activation of the *OCT4* promoter produced additive effects when four gRNAs were pooled with dCas9^{p300Core}, the most potent single gRNA (gRNA “D”) induced a statistically equivalent amount of gene expression to that observed upon co-transfection of dCas9^{VP64} with an equimolar pool of all four promoter gRNAs ($P = 0.73$; Fig. 5c). Compared to dCas9^{p300Core}, gene activation with dCas9^{VP64} and single gRNAs was substantially lower. Also, in contrast to dCas9^{p300Core}, dCas9^{VP64} demonstrated synergistic effects with combinations of gRNAs in every case (Fig. 5a–c), as reported previously^{16,17}.

Based on the transactivation ability of dCas9^{p300Core} at enhancer regions and with single gRNAs at promoter regions, we hypothesized

that dCas9^{p300Core} might also be able to transactivate enhancers by means of a single targeted gRNA. We tested the *MYOD* (DRR and CE), *OCT4* (PE and DE) and HS2 enhancer regions with equimolar concentrations of pooled or individual gRNAs (Fig. 5d–g). For both *MYOD* enhancer regions, co-transfection of dCas9^{p300Core} and a single enhancer-targeting gRNA was sufficient to activate gene expression to levels similar to cells co-transfected with dCas9^{p300Core} and the four pooled enhancer gRNAs (Fig. 5d). Similarly, *OCT4* gene expression was activated from the PE through dCas9^{p300Core} localization with a single gRNA to similar levels as dCas9^{p300Core} localized with a pool of six PE-targeted gRNAs (Fig. 5e). dCas9^{p300Core}-mediated induction of *OCT4* from the DE (Fig. 5e) and *HBE* and *HBG* genes from the HS2 enhancer (Fig. 5f,g) showed increased expression with the pooled gRNAs relative to single gRNAs. Nevertheless, there was activation of target gene expression above control for several single gRNAs at these enhancers (Fig. 5e–g).

The p300 HAT domain is portable to other DNA-binding proteins

The dCas9-gRNA system from *Streptococcus pyogenes* has been widely adopted due to its robust, versatile and easily programmable properties^{9,10}. However, several other programmable DNA-binding proteins are also under development for various applications and may be preferable for particular applications, including orthogonal dCas9 systems from other species⁴⁴, TALEs and zinc finger proteins. To determine if the p300 Core HAT domain was portable to these other systems, we created fusions to dCas9 from *Neisseria meningitidis* (*Nm*-dCas9)⁴⁴, four different TALEs targeting the *IL1RN* promoter²⁴ and a zinc finger protein targeting *ICAM1* (Fig. 6). Co-transfection of *Nm*-dCas9^{p300Core} and five *Nm*-gRNAs targeted to the *HBE* or the *HBG* promoters led

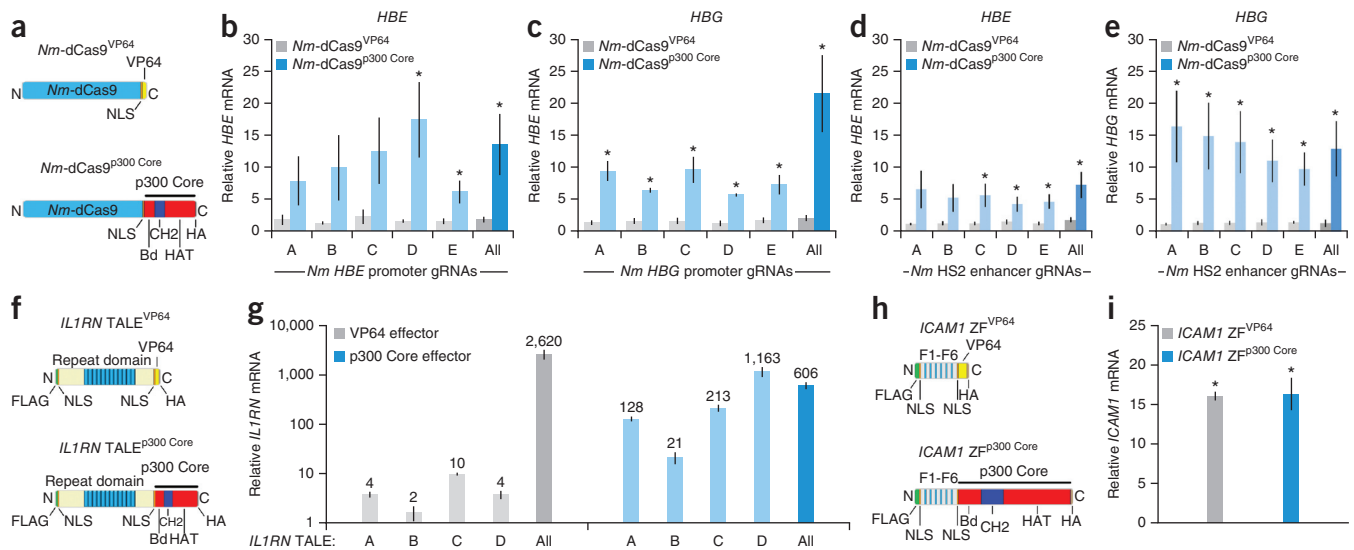


Figure 6 The p300 Core can be targeted to genomic loci by diverse programmable DNA-binding proteins. **(a)** Schematic of the *Neisseria meningitidis* (*Nm*) dCas9 fusion proteins *Nm-dCas9*^{VP64} and *Nm-dCas9*^{p300 Core}. *Neisseria meningitidis* dCas9 contains nuclease-inactivating mutations D16A, D587A, H588A and N611A. **(b,c)** Relative *HBE* **(b)** or *HBG* **(c)** mRNA in cells co-transfected with five individual or pooled (A–E) *Nm* gRNAs targeted to the *HBE* or *HBG* promoter and *Nm-dCas9*^{VP64} or *Nm-dCas9*^{p300 Core}. **(d,e)** Relative *HBE* **(d)** or *HBG* **(e)** mRNA in cells co-transfected with five individual or pooled (A–E) *Nm* gRNAs targeted to the HS2 enhancer and *Nm-dCas9*^{VP64} or *Nm-dCas9*^{p300 Core}. **(f)** Schematic of TALEs with domains containing *IL1RN*-targeted repeat variable di-residues (repeat domain). **(g)** Relative *IL1RN* mRNA in cells transfected with individual or pooled (A–D) *IL1RN* TALE^{VP64} or *IL1RN* TALE^{p300 Core} encoding plasmids. Numbers on top of bars indicate mean relative expression. **(h)** Schematic of ZF fusion proteins with zinc finger helices 1–6 (F1–F6) targeting the *ICAM1* promoter. **(i)** Relative *ICAM1* mRNA in cells transfected with *ICAM1 ZF*^{VP64} or *ICAM1 ZF*^{p300 Core}. Tukey-test, * $P < 0.05$ compared to mock-transfected control, $n = 3$ independent experiments each; error bars, s.e.m. NLS, nuclear localization signal; HA, hemagglutinin tag; Bd, bromodomain; CH, cysteine-histidine-rich region; HAT, histone acetyltransferase domain.

to significant gene induction compared to mock-transfected controls ($P = 0.038$ and 0.0141 for *HBE* and *HBG*, respectively) (Fig. 6b,c). When co-transfected with five *Nm*-gRNAs targeted to the HS2 enhancer, *Nm-dCas9*^{p300 Core} also significantly activated the distal *HBE* and *HBG* globin genes compared to mock-transfected controls ($P = 0.0192$ and $P = 0.0323$, respectively) (Fig. 6d,e). Similar to *dCas9*^{p300 Core}, *Nm-dCas9*^{p300 Core} activated gene expression from promoters and the HS2 enhancer with a single gRNA. *Nm-dCas9*^{VP64} displayed negligible capacity to transactivate *HBE* or *HBG* regardless of localization to promoter regions or to the HS2 enhancer either with single or multiple gRNAs (Fig. 6b–e). Transfection of the expression plasmids for a combination of four TALE^{p300 Core} fusion proteins targeted to the *IL1RN* promoter (*IL1RN TALE*^{p300 Core}) also activated downstream gene expression, although to a lesser extent than four corresponding TALE^{VP64} fusions (*IL1RN TALE*^{VP64}) (Fig. 6f,g). However, single p300 Core effectors were much more potent than single VP64 domains when fused to *IL1RN* TALEs. Interestingly, *dCas9*^{p300 Core} directed to any single binding site generated comparable *IL1RN* expression relative to single or pooled *IL1RN* TALE effectors, and direct comparisons suggest that dCas9 may be a more robust activator than TALEs when fused to the larger p300 Core fusion domain (Supplementary Fig. 5). Finally, the ZF^{p300 Core} fusion targeted to the *ICAM1* promoter (*ICAM1 ZF*^{p300 Core}) also activated its target gene relative to control and at a similar level as ZF^{VP64} (*ICAM1 ZF*^{VP64}) (Fig. 6h,i). The versatility of the p300 Core fusion with multiple targeting domains is evidence that this is a robust approach for targeted acetylation and gene regulation. The various p300 core fusion proteins were expressed well, as determined by western blot analysis (Supplementary Fig. 6), but differences in p300 Core activity between different fusion proteins could be attributable to binding affinity or protein folding.

DISCUSSION

These results establish the *dCas9*^{p300 Core} fusion protein as a potent and easily programmable tool to synthetically manipulate acetylation at targeted endogenous loci, leading to regulation of proximal and distal enhancer-regulated genes. The intrinsic p300 Core acetyltransferase activity is crucial for this efficacy, as demonstrated by the consistent lack of chromatin modification and transactivation potential of the *dCas9*^{p300 Core} (D1399Y) acetyltransferase-null mutant (Figs. 1c, 2c and 4b–d and Supplementary Fig. 1). Fusion of the catalytic core domain of p300 to dCas9 resulted in substantially higher transactivation of downstream genes than the direct fusion of full-length p300 protein despite robust protein expression (Fig. 1b,c). This may be due to differences in protein structure and function or interactions with other cellular proteins, suggesting that isolation of catalytic core regions is a useful strategy for future programmable epigenome editing tools. The *dCas9*^{p300 Core} fusion protein also had an increased transactivation capacity relative to *dCas9*^{VP64} (Figs. 1c, 2, 3 and 5), including in the context of the *Nm-dCas9* scaffold (Fig. 6b–e). This was especially evident at distal enhancer regions, at which *dCas9*^{VP64} displayed little, if any, measurable downstream transcriptional activity (Figs. 2 and 6d,e). In addition, the *dCas9*^{p300 Core} displayed precise and robust genome-wide transcriptional specificity (Fig. 3 and Supplementary Fig. 2).

The observation that targeted acetylation is sufficient for gene activation at an endogenous locus and enhancer is a notable finding of our study. Although it is possible that activation or recruitment of other co-factors is involved in the targeted *dCas9*^{p300 Core}-mediated epigenomic control, only *dCas9*^{p300 Core} and not VP64 was capable of potent transcriptional activation and co-enrichment of acetylation at promoters targeted by the epigenetically modified enhancer (Figs. 2c and 3c,d and Supplementary Fig. 3). The two

effector domains have different modes of activity; whereas p300 has inherent acetyltransferase activity^{29,30}, VP64 relies upon sequential recruitment of co-factors, including endogenous p300, for HAT activity at sites of transactivation^{27,28}. Thus, our results support a model in which acetylation is a sufficient step in activating enhancer activity, at least at the loci tested here.

The unique activity of dCas9^{p300 Core} supports its use in elucidating key steps of gene regulation, including dissection of the interplay between the epigenome, regulatory element activity and gene regulation. For example, the GATA1 transcription factor that is essential for globin gene expression in erythroid cells⁴⁵ is not expressed in the HEK293T cells used in this study¹⁶. The observed potent activation of globin gene expression by dCas9^{p300 Core}-mediated acetylation in the absence of GATA1 suggests that the acetylation at the enhancer occurs downstream of GATA1 but upstream of globin gene activation in erythroid cells. Notably, the greater transactivation potency of direct acetylation by dCas9^{p300 Core} relative to dCas9^{VP64} suggests that acetylation of additional factors at the target site may also play a role, and this should be a subject of future investigation.

dCas9^{p300 Core} is more potent than existing engineered transcription factors made with single activator domains. Although synergy among other synthetic transcriptional activators, including dCas9^{VP64} (refs. 8,15–17,19–22,24,25), has been widely observed, the p300 Core effector domain did not display similar synergy with either additional gRNAs or TALEs (Figs. 5 and 6 and Supplementary Figs. 3 and 5) or in combination with VP64 (Supplementary Fig. 7). Moreover, the p300 Core effector was capable of robustly activating gene expression through a single gRNA at promoters and characterized enhancers (Figs. 5 and 6 and Supplementary Fig. 3). This effector was also capable of potent gene activation when targeted by a single TALE recognition site (Fig. 6 and Supplementary Fig. 5). Notably, certain loci appear to be less responsive to transactivation by the localization of a single dCas9^{p300 Core} effector to a corresponding regulatory region (Fig. 5e–g and Supplementary Fig. 3). This does not appear to be related to chromatin accessibility based on ENCODE data (Supplementary Fig. 8), but may be related to transcription factor occupancy or competition (including endogenous p300; Supplementary Figs. 3 and 8), gRNA and genetic composition⁴⁶, transcription start site proximity¹⁴, and/or the underlying local epigenetic circuitry, none of which are mutually exclusive. These factors are relevant to the function of all programmable DNA-binding proteins and their effects may be mitigated by the use of optimal gRNAs.

Our results indicate a causal relationship between directed acetylation and subsequent target-gene activation. The technology affords the ability to synthetically transactivate distal genes from putative and known regulatory regions and simplifies transactivation by the application of a single programmable effector and single target site. These capabilities could be important in enabling genome-wide screens of regulatory element activity and in multiplexing to target several promoters and/or enhancers simultaneously^{14,20,47}. Furthermore combining dCas9^{p300 Core} with light-inducible^{7,48} or chemically inducible⁴⁹ control would permit dynamic control of gene activation in space and time. The ability to target the p300 Core domain with orthogonal dCas9s, TALEs and zinc finger proteins should facilitate studies of independent targeting of particular effector functions to distinct loci (Fig. 5 and Supplementary Fig. 3). This could include multiplexing of various activators, repressors and epigenetic modifiers to precisely control cell phenotype^{23,33,50} or decipher complex networks of gene regulation. In addition, the mammalian origin of p300 may provide advantages over virally derived effector domains for *in vivo* applications by minimizing potential immunogenicity.

The synthetic control of transcription and chromatin remodeling is a critical component of cellular engineering. dCas9^{p300 Core} takes advantage of the simple programmability of the CRISPR-Cas9 system to target acetyltransferase activity and complements other recently described epigenetic editing tools, including fusions of demethylases, methyltransferases and deacetylases^{3–7} to generate a more complete set of epigenome editing tools.

METHODS

Methods and any associated references are available in the [online version of the paper](#).

Accession codes. GEO: [GSE66742](#).

Note: Any Supplementary Information and Source Data files are available in the online version of the paper.

ACKNOWLEDGMENTS

P. Perez-Pinera, D. Kocak, D. Ousterout and D. Lim provided assistance with gRNA design, plasmid cloning, PCR primer validation, and/or RNA isolations. The gene encoding the *ICAM1*-targeted zinc finger protein was provided by C. Barbas, III. This work was supported by a US National Institutes of Health (NIH) grants to G.E.C., C.A.G. and T.E.R. (R01DA036865 and U01HG007900), a NIH Director's New Innovator Award (DP2OD008586) and National Science Foundation (NSF) Faculty Early Career Development (CAREER) Award (CBET-1151035) to C.A.G. and NIH grant P30AR066527.

AUTHOR CONTRIBUTIONS

I.B.H., A.M.D., C.M.V., P.I.T., G.E.C., T.E.R. and C.A.G. designed experiments. I.B.H., A.M.D. and C.M.V. performed the experiments. I.B.H., A.M.D., C.M.V., P.I.T., G.E.C., T.E.R. and C.A.G. analyzed the data. I.B.H. and C.A.G. wrote the manuscript with contributions by all authors.

COMPETING FINANCIAL INTERESTS

The authors declare competing financial interests: details are available in the [online version of the paper](#).

Reprints and permissions information is available online at <http://www.nature.com/reprints/index.html>.

1. ENCODE Project Consortium. An integrated encyclopedia of DNA elements in the human genome. *Nature* **489**, 57–74 (2012).
2. Bernstein, B.E. *et al.* The NIH Roadmap Epigenomics Mapping Consortium. *Nat. Biotechnol.* **28**, 1045–1048 (2010).
3. Snowden, A.W., Gregory, P.D., Case, C.C. & Pabo, C.O. Gene-specific targeting of H3K9 methylation is sufficient for initiating repression *in vivo*. *Curr. Biol.* **12**, 2159–2166 (2002).
4. Maeder, M.L. *et al.* Targeted DNA demethylation and activation of endogenous genes using programmable TALE-TET1 fusion proteins. *Nat. Biotechnol.* **31**, 1137–1142 (2013).
5. Mendenhall, E.M. *et al.* Locus-specific editing of histone modifications at endogenous enhancers. *Nat. Biotechnol.* **31**, 1133–1136 (2013).
6. Rivenbark, A.G. *et al.* Epigenetic reprogramming of cancer cells via targeted DNA methylation. *Epigenetics* **7**, 350–360 (2012).
7. Konermann, S. *et al.* Optical control of mammalian endogenous transcription and epigenetic states. *Nature* **500**, 472–476 (2013).
8. Keung, A.J., Bashor, C.J., Kiriakov, S., Collins, J.J. & Khalil, A.S. Using targeted chromatin regulators to engineer combinatorial and spatial transcriptional regulation. *Cell* **158**, 110–120 (2014).
9. Hsu, P.D., Lander, E.S. & Zhang, F. Development and applications of CRISPR-Cas9 for genome engineering. *Cell* **157**, 1262–1278 (2014).
10. Doudna, J.A. & Charpentier, E. Genome editing. The new frontier of genome engineering with CRISPR-Cas9. *Science* **346**, 1258096 (2014).
11. Mali, P. *et al.* RNA-guided human genome engineering via Cas9. *Science* **339**, 823–826 (2013).
12. Jinek, M. *et al.* A programmable dual-RNA-guided DNA endonuclease in adaptive bacterial immunity. *Science* **337**, 816–821 (2012).
13. Cong, L. *et al.* Multiplex genome engineering using CRISPR/Cas systems. *Science* **339**, 819–823 (2013).
14. Konermann, S. *et al.* Genome-scale transcriptional activation by an engineered CRISPR-Cas9 complex. *Nature* **517**, 583–588 (2015).
15. Mali, P. *et al.* CAS9 transcriptional activators for target specificity screening and paired nickases for cooperative genome engineering. *Nat. Biotechnol.* **31**, 833–838 (2013).

16. Perez-Pinera, P. *et al.* RNA-guided gene activation by CRISPR-Cas9-based transcription factors. *Nat. Methods* **10**, 973–976 (2013).
17. Maeder, M.L. *et al.* CRISPR RNA-guided activation of endogenous human genes. *Nat. Methods* **10**, 977–979 (2013).
18. Qi, L.S. *et al.* Repurposing CRISPR as an RNA-guided platform for sequence-specific control of gene expression. *Cell* **152**, 1173–1183 (2013).
19. Gilbert, L.A. *et al.* CRISPR-mediated modular RNA-guided regulation of transcription in eukaryotes. *Cell* **154**, 442–451 (2013).
20. Cheng, A.W. *et al.* Multiplexed activation of endogenous genes by CRISPR-on, an RNA-guided transcriptional activator system. *Cell Res.* **23**, 1163–1171 (2013).
21. Farzadfard, F., Perli, S.D. & Lu, T.K. Tunable and multifunctional eukaryotic transcription factors based on CRISPR/Cas. *ACS Synth. Biol.* **2**, 604–613 (2013).
22. Tanenbaum, M.E., Gilbert, L.A., Qi, L.S., Weissman, J.S. & Vale, R.D. A protein-tagging system for signal amplification in gene expression and fluorescence imaging. *Cell* **159**, 635–646 (2014).
23. Chavez, A. *et al.* Highly efficient Cas9-mediated transcriptional programming. *Nat. Methods* doi:10.1038/nmeth.3312 (2 March 2015).
24. Perez-Pinera, P. *et al.* Synergistic and tunable human gene activation by combinations of synthetic transcription factors. *Nat. Methods* **10**, 239–242 (2013).
25. Maeder, M.L. *et al.* Robust, synergistic regulation of human gene expression using TALE activators. *Nat. Methods* **10**, 243–245 (2013).
26. Beerli, R.R., Dreier, B. & Barbas, C.F. III. Positive and negative regulation of endogenous genes by designed transcription factors. *Proc. Natl. Acad. Sci. USA* **97**, 1495–1500 (2000).
27. Choy, B. & Green, M.R. Eukaryotic activators function during multiple steps of preinitiation complex assembly. *Nature* **366**, 531–536 (1993).
28. Memedula, S. & Belmont, A.S. Sequential recruitment of HAT and SWI/SNF components to condensed chromatin by VP16. *Curr. Biol.* **13**, 241–246 (2003).
29. Delvecchio, M., Gaucher, J., Aguilar-Gurreri, C., Ortega, E. & Panne, D. Structure of the p300 catalytic core and implications for chromatin targeting and HAT regulation. *Nat. Struct. Mol. Biol.* **20**, 1040–1046 (2013).
30. Ogryzko, V.V., Schiltz, R.L., Russanova, V., Howard, B.H. & Nakatani, Y. The transcriptional coactivators p300 and CBP are histone acetyltransferases. *Cell* **87**, 953–959 (1996).
31. Chen, J. & Li, Q. Life and death of transcriptional co-activator p300. *Epigenetics* **6**, 957–961 (2011).
32. Gao, X. *et al.* Comparison of TALE designer transcription factors and the CRISPR/dCas9 in regulation of gene expression by targeting enhancers. *Nucleic Acids Res.* **42**, e155 (2014).
33. Gao, X. *et al.* Reprogramming to pluripotency using designer TALE transcription factors targeting enhancers. *Stem Cell Reports* **1**, 183–197 (2013).
34. Ji, Q. *et al.* Engineered zinc-finger transcription factors activate OCT4 (POU5F1), SOX2, KLF4, c-MYC (MYC) and miR302/367. *Nucleic Acids Res.* **42**, 6158–6167 (2014).
35. Deng, W. *et al.* Reactivation of developmentally silenced globin genes by forced chromatin looping. *Cell* **158**, 849–860 (2014).
36. Rada-Iglesias, A. *et al.* A unique chromatin signature uncovers early developmental enhancers in humans. *Nature* **470**, 279–283 (2011).
37. Visel, A. *et al.* ChIP-seq accurately predicts tissue-specific activity of enhancers. *Nature* **457**, 854–858 (2009).
38. Chen, J.C., Love, C.M. & Goldhamer, D.J. Two upstream enhancers collaborate to regulate the spatial patterning and timing of MyoD transcription during mouse development. *Dev. Dyn.* **221**, 274–288 (2001).
39. Nordhoff, V. *et al.* Comparative analysis of human, bovine, and murine Oct-4 upstream promoter sequences. *Mamm. Genome* **12**, 309–317 (2001).
40. Carter, D., Chakalova, L., Osborne, C.S., Dai, Y.F. & Fraser, P. Long-range chromatin regulatory interactions *in vivo*. *Nat. Genet.* **32**, 623–626 (2002).
41. Kim, Y.W. & Kim, A. Histone acetylation contributes to chromatin looping between the locus control region and globin gene by influencing hypersensitive site formation. *Biochim. Biophys. Acta* **1829**, 963–969 (2013).
42. Kucus, C., Arslan, S., Singh, R., Thorpe, J. & Adli, M. Genome-wide analysis reveals characteristics of off-target sites bound by the Cas9 endonuclease. *Nat. Biotechnol.* **32**, 677–683 (2014).
43. Wu, X. *et al.* Genome-wide binding of the CRISPR endonuclease Cas9 in mammalian cells. *Nat. Biotechnol.* **32**, 670–676 (2014).
44. Esvelt, K.M. *et al.* Orthogonal Cas9 proteins for RNA-guided gene regulation and editing. *Nat. Methods* **10**, 1116–1121 (2013).
45. Su, M.Y. *et al.* Identification of biologically relevant enhancers in human erythroid cells. *J. Biol. Chem.* **288**, 8433–8444 (2013).
46. Doench, J.G. *et al.* Rational design of highly active sgRNAs for CRISPR-Cas9-mediated gene inactivation. *Nat. Biotechnol.* **32**, 1262–1267 (2014).
47. Gilbert, L.A. *et al.* Genome-scale CRISPR-mediated control of gene repression and activation. *Cell* **159**, 647–661 (2014).
48. Polstein, L.R. & Gersbach, C.A. A light-inducible CRISPR-Cas9 system for control of endogenous gene activation. *Nat. Chem. Biol.* **11**, 198–200 (2015).
49. Zetsche, B., Volz, S.E. & Zhang, F. A split-Cas9 architecture for inducible genome editing and transcription modulation. *Nat. Biotechnol.* **33**, 139–142 (2015).
50. Chakraborty, S. *et al.* A CRISPR-Cas9-based system for reprogramming cell lineage specification. *Stem Cell Reports* **3**, 940–947 (2014).

ONLINE METHODS

Cell lines and transfection. HEK293T cells were procured from the American Tissue Collection Center (ATCC, Manassas, VA) through the Duke University Cell Culture Facility. Cells were cultured in Dulbecco's modified Eagle's medium (DMEM) supplemented with 10% FBS and 1% penicillin/streptomycin and maintained at 37 °C and 5% CO₂. Transfections were performed in 24-well plates using 375 ng of respective dCas9 expression vector and 125 ng of equimolar pooled or individual gRNA expression vectors mixed with Lipofectamine 2000 (Life Technologies, cat. #11668019) as per manufacturer's instruction. For ChIP-qPCR experiments, HEK293T cells were transfected in 15-cm dishes with Lipofectamine 2000 and 30 µg of respective dCas9 expression vector and 10 µg of equimolar pooled gRNA expression vectors as per manufacturer's instruction.

Plasmid constructs. pcDNA-dCas9^{VP64} (dCas9^{VP64}; Addgene, plasmid #47107) has been described previously¹⁶. An HA epitope tag was added to dCas9 (no effector) by removing the VP64 effector domain from dCas9^{VP64} via *AscI*/*PacI* restriction sites and using isothermal assembly⁵¹ to include an annealed set of oligos containing the appropriate sequence as per manufacturer's instruction (NEB cat. #2611). pcDNA-dCas9^{FLp300} (dCas9^{FLp300}) was created by amplifying full-length p300 from pcDNA3.1-p300 (Addgene, plasmid #23252)⁵² in two separate fragments and cloning these fragments into the dCas9^{VP64} backbone via isothermal assembly. A substitution in the full-length p300 protein (L553M), located outside of the HAT Core region, was identified in dCas9^{FLp300} and in the precursor pcDNA3.1-p300 during sequence validation. pcDNA-dCas9^{p300 Core} (dCas9^{p300 Core}) was generated by first amplifying amino acids 1,048–1,664 of human p300 from cDNA and then subcloning the resulting amplicon into pCR-Blunt (pCR-Blunt^{p300 Core}) (Life Technologies cat. #K2700). An *AscI* site, HA-epitope tag, and a *PmeI* site were added by PCR amplification of the p300 Core from pCR-Blunt^{p300 Core}, and subsequently this amplicon was cloned into pCR-Blunt (pCR-Blunt^{p300 Core + HA}) (Life Technologies cat. #K2700). The HA-tagged p300 Core was cloned from pCR-Blunt^{p300 Core + HA} into the dCas9^{VP64} backbone via shared *AscI*/*PmeI* restriction sites. pcDNA-dCas9^{p300 Core (D1399Y)} (dCas9^{p300 Core (D1399Y)}) was generated by amplification of the p300 Core from dCas9^{p300 Core} in overlapping fragments with primer sets including the specified nucleic acid mutations, with a subsequent round of linkage PCR and cloning into the dCas9^{p300 Core} backbone using shared *AscI*/*PmeI* restriction sites. All PCR amplifications were carried out using Q5 high-fidelity DNA polymerase (NEB cat. #M0491). Protein sequences of all dCas9 constructs are shown in **Supplementary Note 1**.

ILIRN, *MYOD* and *OCT4* promoter gRNA protospacers have been described previously^{16,53}. *Neisseria meningitidis* dCas9^{VP64} (*Nm*-dCas9^{VP64}) was obtained from Addgene (plasmid #48676)⁴⁴. *Nm*-dCas9^{p300 Core} was created by amplifying the HA-tagged p300 Core from dCas9^{p300 Core} with primers to facilitate subcloning into the *Al**I*/*AgeI*-digested *Nm*-dCas9^{VP64} backbone using isothermal assembly (NEB cat. #2611). *ILIRN* TALE^{p300 Core} TALEs were generated by subcloning the HA-tagged p300 Core domain from dCas9^{p300 Core} into previously published²⁴ *ILIRN* TALE^{VP64} constructs via shared *AscI*/*PmeI* restriction sites. *ILIRN* TALE target sites are shown in **Supplementary Table 2**. *ICAM1* ZF^{VP64} and *ICAM1* ZF^{p300 Core} were constructed by subcloning the *ICAM1* ZF from pMX-CD54-31Opt-VP64 (ref. 54) into dCas9^{VP64} and dCas9^{p300 Core} backbones, respectively, using isothermal assembly (NEB cat. #2611). Protein sequences of *ICAM1* ZF constructs are shown in **Supplementary Note 2**. Transfection efficiency was routinely above 90% as assayed by co-transfection of PL-SIN-EF1 α -EGFP (Addgene plasmid #21320)⁵⁵ and gRNA empty vector in all experiments. All *S. pyogenes* gRNAs were annealed and cloned into pZdonor-pSPgRNA (Addgene plasmid #47108)¹⁶ for expression as described previously¹³ with slight modifications using NEB *BbsI* and T4 ligase (Cat. #s R0539 and M0202). *Nm*-dCas9 gRNA oligos were rationally designed using published PAM requirements⁴⁴, and then cloned into pZdonor-Nm-Cas9-gRNA-hU6 (Addgene, plasmid #61366) via *BbsI* sites. Plasmids are available through Addgene (**Supplementary Table 3**). All gRNA protospacer targets are listed in **Supplementary Table 4**.

Western blot analysis. 20 µg of protein was loaded for SDS PAGE and transferred onto a nitrocellulose membrane for western blots. Primary antibodies

(α -FLAG; Sigma-Aldrich cat. #F7425 and α -GAPDH; Cell Signaling Technology cat. #14C10) were used at a 1:1,000 dilution in TBST + 5% milk. Secondary α -Rabbit HRP (Sigma-Aldrich cat. #A6154) was used at a 1:5,000 dilution in TBST + 5% milk. Membranes were exposed after addition of ECL (Bio-Rad cat. #170-5060).

Quantitative reverse-transcription PCR. RNA was isolated from transfected cells using the RNeasy Plus mini kit (Qiagen cat. #74136) and 500 ng of purified RNA was used as template for cDNA synthesis (Life Technologies, cat. #11754). Real-time PCR was performed using PerFeCTa SYBR Green FastMix (Quanta Biosciences, cat. #95072) and a CFX96 Real-Time PCR Detection System with a C1000 Thermal Cycler (Bio-Rad). Baselines were subtracted using the baseline subtraction curve fit analysis mode and thresholds were automatically calculated using the Bio-Rad CFX Manager software version 2.1. Results are expressed as fold change above control mock transfected cells (no DNA) after normalization to GAPDH expression using the $\Delta\Delta$ Ct method, as previously described⁵⁶. All qPCR primers and conditions are listed in **Supplementary Table 5**.

RNA-seq. RNA-seq was performed using three replicates per experimental condition. RNA was isolated from transfected cells using the RNeasy Plus mini kit (Qiagen cat. #74136) and 1 µg of purified mRNA was used as template for cDNA synthesis and library construction using the PrepX RNA-Seq Library Kit (Wafergen Biosystems, cat. #400039). Libraries were prepared using the Apollo 324 liquid handling platform, as per manufacturer's instruction. Indexed libraries were validated for quality and size distribution using the TapeStation 2200 (Agilent) and quantified by qPCR using the KAPA Library Quantification Kit (KAPA Biosystems; KK4835) before multiplex pooling and sequencing at the Duke University Genome Sequencing Shared Resource facility. Libraries were pooled and then 50-bp single-end reads were sequenced on a HiSeq 2500 (Illumina), de-multiplexed and then aligned to the HG19 transcriptome using Bowtie 2 (ref. 57). Transcript abundance was calculated using the SAMtools⁵⁸ suite, and differential expression was determined in R using the DESeq2 analysis package. Multiple hypothesis correction was performed using the method of Benjamini and Hochberg with a FDR of < 5%.

ChIP-qPCR. HEK293T cells were co-transfected with four HS2 enhancer gRNA constructs and indicated dCas9 fusion expression vectors in 15-cm plates in biological triplicate for each condition tested. Cells were cross-linked with 1% formaldehyde (final concentration; Sigma F8775-25ML) for 10 min at RT and then the reaction was stopped by the addition of glycine to a final concentration of 125 mM. From each plate ~2.5e7 cells were used for H3K27ac ChIP-enrichment. Chromatin was sheared to a median fragment size of 250 bp using a Bioruptor XL (Diagenode). H3K27ac enrichment was performed by incubation with 5 µg of Abcam ab4729 and 200 µl of sheep anti-rabbit IgG magnetic beads (Life Technologies 11203D) for 16 h at 4 °C. Cross-links were reversed via overnight incubation at 65 °C with sodium dodecyl sulfate, and DNA was purified using MinElute DNA purification columns (Qiagen). 10 ng of DNA was used for subsequent qPCR reactions using a CFX96 Real-Time PCR Detection System with a C1000 Thermal Cycler (Bio-Rad). Baselines were subtracted using the baseline subtraction curve fit analysis mode and thresholds were automatically calculated using the Bio-Rad CFX Manager software version 2.1. Results are expressed as fold change above cells co-transfected with dCas9 and four HS2 gRNAs after normalization to β -actin enrichment using the $\Delta\Delta$ Ct method as previously described⁵⁶. All ChIP-qPCR primers and conditions are listed in **Supplementary Table 5**.

51. Gibson, D.G. *et al.* Enzymatic assembly of DNA molecules up to several hundred kilobases. *Nat. Methods* **6**, 343–345 (2009).

52. Chen, L.F., Mu, Y. & Greene, W.C. Acetylation of RelA at discrete sites regulates distinct nuclear functions of NF-kappaB. *EMBO J.* **21**, 6539–6548 (2002).

53. Hu, J. *et al.* Direct activation of human and mouse Oct4 genes using engineered TALE and Cas9 transcription factors. *Nucleic Acids Res.* **42**, 4375–4390 (2014).

54. Magnenat, L., Blancafort, P. & Barbas, C.F. III. In vivo selection of combinatorial libraries and designed affinity maturation of polydactyl zinc finger transcription factors for ICAM-1 provides new insights into gene regulation. *J. Mol. Biol.* **341**, 635–649 (2004).

55. Hotta, A. *et al.* Isolation of human iPS cells using EOS lentiviral vectors to select for pluripotency. *Nat. Methods* **6**, 370–376 (2009).
56. Schmittgen, T.D. & Livak, K.J. Analyzing real-time PCR data by the comparative C(T) method. *Nat. Protoc.* **3**, 1101–1108 (2008).
57. Langmead, B. & Salzberg, S.L. Fast gapped-read alignment with Bowtie 2. *Nat. Methods* **9**, 357–359 (2012).
58. Li, H. *et al.* The Sequence Alignment/Map format and SAMtools. *Bioinformatics* **25**, 2078–2079 (2009).

